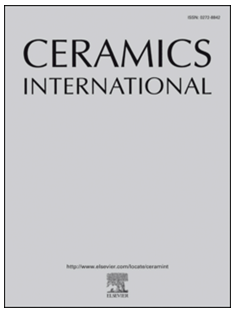

The controlled preparation and stability mechanism of partially stabilized zirconia by microwave intensification

Kangqiang Li, Qi Jiang, Jin Chen, Jinhui Peng, Xinpei Li, Sivasankar Koppala, Mamdouh Omran, Guo Chen

PII: S0272-8842(19)33444-3

DOI: https://doi.org/10.1016/j.ceramint.2019.11.251

Reference: CERI 23620

To appear in: *Ceramics International*

Received Date: 9 November 2019

Revised Date: 23 November 2019

Accepted Date: 27 November 2019

Please cite this article as: K. Li, Q. Jiang, J. Chen, J. Peng, X. Li, S. Koppala, M. Omran, G. Chen, The controlled preparation and stability mechanism of partially stabilized zirconia by microwave intensification, *Ceramics International* (2019), doi: https://doi.org/10.1016/j.ceramint.2019.11.251.

The controlled preparation and stability mechanism of partially stabilized zirconia by microwave intensification

Kangqiang Li [a], Qi Jiang [a], Jin Chen [a, b, **], Jinhui Peng [a, b], Xinpei Li [a], Sivasankar Koppala [a], Mamdouh Omran [c], Guo Chen [a, b, *]

[a] *Faculty of Metallurgical and Energy Engineering, Kunming University of Science and Technology, Kunming 650093, P.R. China.*

[b] *Key Laboratory of Green-Chemistry Materials in University of Yunnan Province, Kunming Key Laboratory of Energy Materials Chemistry, Yunnan Minzu University, Kunming 650500, P.R. China.*

[c] *Process Metallurgy Research Group, Faculty of Technology, University of Oulu, Finland.*

[*] Corresponding author:

E-mail address: guochen@kust.edu.cn

[**] Co-Corresponding author:

E-mail address: jinchen@kust.edu.cn

Abstract:

Partially stabilized zirconia (PSZ) occupies an important application portion in ceramics materials and refractories materials. In this work, calcium oxide-partially stabilized zirconia (CaO-PSZ) ceramics were prepared from fused zirconia by microwave sintering, with its

microstructure and stability properties characterized by XRD and SEM. Results indicated that the heating rate, cooling rate, quenching temperature and isothermal treatment time rendered different influence on the stability properties, which was mainly ascribed to the reversible martensitic transformation of zirconia ceramics. Additionally, a mixed-phase composed by cubic phase ZrO_2 (c-ZrO_2) and monoclinic phase ZrO_2 (m-ZrO_2) appeared after fused zirconia treated by microwave sintering at 1450 °C for 2 h, indicating the formation of CaO-PSZ ceramics, which the finding was consistent with the SEM and EDAX analysis. Meanwhile, CaO stabilizer precipitated behavior at the crystal boundary, with the formation of acicular grains and fine particles, further rendering a toughening effect to CaO-PSZ ceramics. This work can provide important theoretical and practical significance for applications of microwave sintering to prepare CaO-PSZ ceramics material, even extending further applications in functional materials and structural materials.

Keywords: CaO-PSZ ceramics; fused zirconia; microwave sintering; structure

1 Introduction

Zirconia (ZrO_2) has outstood in the fields of advanced ceramics materials, such as bio-ceramics, electronic ceramics, functional ceramics and structural ceramics [1-3], attributed to its outstanding functional properties, including high melting point, strong corrosion resistance and high-temperature resistance, high chemical inertness and low thermal conductivity [4-5]. Additionally, it has widespreadly applied in high-temperature insulation materials, high-temperature refractory materials, and abrasive materials [6-8]. However, in the preparation process of zirconia ceramics materials, a large volume effect occurs with

temperature rising or falling, accompanied with the internal stress accumulated and the defects formed, generating the fatal influence on the thermomechanical properties of zirconia ceramics and further severely limiting the further applications in functional materials and structural materials [9, 10].

Zirconia (ZrO_2) endows the unique martensitic transformation characteristic, representing by the three crystal phases undergo these reversible phase changes with temperature changes: m-ZrO_2 ↔ t-ZrO_2 ↔ c-ZrO_2 [11,12], wherein the monoclinic phase (m-ZrO_2) is converted to tetragonal phase (t-ZrO_2) at 1173 °C, with the reversible transformation phase transition occurred at 1000 °C, and tetragonal phase (t-ZrO_2) is converted into cubic phase (c-ZrO_2) at 2370 °C [13]. The fine precipitates of monoclinic zirconia in a stable cubic matrix in partially stabilized zirconia (PSZ) greatly improved the toughness and thermal shock resistance properties of ceramic materials and refractory materials, discovered by Garvie et al. [14], which the discovery significantly promoted the expansion of the applications of zirconia materials. Currently, partially stabilized zirconia (PSZ) ceramics is mainly manufactured by doping with metal oxides into fused zirconia, such as CaO [15], MgO [16], Al_2O_3 [17], Bi_2O_3 [18], CeO_2 [19], and Y_2O_3 [20]. Through doping treatment, a cation in the metal oxides with a larger radius than Zr^{4+} cation is introduced to replace the position of Zr^{4+} ion, thus rendering the formation of the stable replacement solid solution [21, 22], further to achieve the toughening effect for zirconia ceramics materials by the stable phase structure preserved at room temperature [23, 24]. Garvie et al. have reported the successful preparation of the calcium-doped partially stabilized zirconia (CaO-PSZ) ceramics at 1750 °C for 5 h in a conventional furnace [22]. Apparently, during the

conventional preparation process, the roasting temperature was high and the working time was long, even with the low controllability of product quality, rendering the industrial production of partially stabilized zirconia (PSZ) ceramics materials was blocked. Therefore, it is increasingly urgent to develop new preparation processes for partially stabilized zirconia (PSZ) ceramics, aiming to overcome the technical problems.

The flexible applications of microwave heating instead of conventional heating have been reported continuously, in the fields of material preparation, chemical synthesis, and mineral processing, etc. [25-27], attributed to its unique heating characteristics, including selective heating, volumetric heating, clean production and pollution-free, operation timely and responsive [28-30]. Guo et al. reported the fused zirconia endowed excellent microwave-absorbing properties, taking within 5 min to be heated to 1500 °C [31]; meanwhile, the further study indicated the partially stabilized zirconia (PSZ) ceramics could be prepared from fused zirconia by microwave sintering at 1450 °C for 4 h, and the crystal form and stability of zirconia could be controlled, achieving the rapid, efficient, energy-saving and environmentally friendly production processes [32]. Zhang et al. utilized microwave sintering to efficiently prepare the CaO-doped PSZ ceramics material, at a lower temperature of 950 °C even with holding time less than 4 h [33]. Mazaheri et al. utilized the conventional sintering and microwave sintering to process nanocrystalline yttria-stabilized zirconia, and the results indicated the microwave-treated samples had the very fine grain sizes and macroscopic mechanical properties, exhibiting better microstructure uniformity [34]. Thridandapani et al. reported a reduction of 300 °C in temperature for full densification of 8 mol% yttria–zirconia (8YZ) was achieved by direct microwave sintering

compared with conventional sintering, and even 100 °C lower than microwave-hybrid sintering with no difference in resulting properties [35]. Microwave heating directly delivery the required energy to reaction atoms to form the unique mechanism of microwave heating, instead of the conventional heating through heat transfer process from the surface to inside [36-38], changing the gradient direction of some migration potentials during the conventional heating process, achieving the volumetric heating of the sample with a fast heating rate and uniform heating, further to cause the formation of a microscopic structure with small particle size and uniform distribution [39-40], rendering the excellent effects for zirconia ceramics materials by microwave sintering.

In this work, calcium oxide-partially stabilized zirconia (CaO-PSZ) ceramics was prepared from fused zirconia by microwave sintering to replace conventional sintering. Meanwhile, the effects of heating rate, cooling rate, quenching temperature and isothermal treatment time on stability properties of the prepared CaO-PSZ ceramics samples were investigated. Moreover, the phase transformation and microstructure properties of fused zirconia and the prepared CaO-PSZ ceramics samples by microwave sintering were comparatively analyzed by XRD, SEM and EDAX.

2 Materials and methods

2.1 Materials

The fused zirconia was utilized as the raw material to synthesize partially stabilized zirconia (PSZ) ceramics; and the fused zirconia material is categorized as the full stabilized zirconia (FSZ) ceramics, received from a factory in Yingkou City (Liaoning Province, P.R.

China). The component analysis results of fused zirconia were as follows (%/(w/w): ZrO_2, 95.1; CaO, 3.8; SiO_2, 0.4; Al_2O_3, 0.3; TiO_2, 0.2; Fe_2O_3, 0.1, respectively. Based on the component analysis, it can be concluded that the fused zirconia was mainly composed by 95.1% of ZrO_2 and 3.8% of CaO stabilizer, accompanied by some low-content gangue and metal oxides.

The phase structure of fused zirconia was determined by XRD characterization, and the pattern was plotted in Fig. 1. As shown in Fig. 1, only cubic phase zirconia (c-ZrO_2, JCPDS: 49-1642) existed in the fused zirconia, verifying the fused zirconia belonged to full stabilized zirconia (FSZ). Meanwhile, combining with the component analysis and XRD characterization, wherein the component analysis indicated CaO stabilizer existed in fused zirconia, while the diffraction peaks of calcium oxide (CaO) were not detected by XRD; therefore, it can be concluded that CaO stabilizer completely dissolved in the fused zirconia to form a solid solution.

2.2 Characterization

The characterized zirconia ceramics samples included the fused zirconia raw material and the CaO-PSZ ceramics prepared by microwave sintering. Wherein the crystal structures of zirconia samples were characterized by X-ray diffraction (D/Max 2500, Rigaku, Japan) with CuKα Radiation analysis, and the stability properties of zirconia samples were analyzed based on the corresponded XRD patterns; additionally, the microscopic appearance of zirconia samples were performed using Scanning electron microscopy (XL30ESEM-TMP, Philips, Holland). Meanwhile, the attached Energy dispersion scanner spectrometer (EDAX) was utilized to determine the elemental semi-quantitative analysis of zirconia samples.

2.3 Instrumentation

The sintering preparation experiments for CaO-doped partially stabilized zirconia (CaO-PSZ) ceramics were performed in a box-type microwave high temperature furnace (HM-X08-16). The schematic diagram of microwave high temperature furnace was illustrated in Fig. 2. As presented in Fig. 2, the microwave furnace mainly consisted of microwave reactor, vacuum pump, infrared thermocouple, rotation, motor, insulating brick, a computer control system, a weight measurement system, barometer, rotameter, flowmeter and gas generator. The protective gas was injected into the reactor cavity based on the experimental need. The temperature was measured by an infrared thermocouple (Marathon Series, Raytek, USA), with a maximum service temperature of 1600 °C. Microwave power with a continuous controllable regime of 0-3 kW was supplied by two magnetrons at 2.45 GHz microwave frequency for different experimental demand.

2.4 Procedure

Fused zirconia raw material was crushed to powder with a particle size of 10-20 mm, and then 100.0 g of the ground fused zirconia was weighed by an electronic balance (Tricle-QD-1) and introduced into a ceramic crucible and sintered by the box-type microwave high temperature furnace (HM-X08-16). During the preparation process of partially stabilized zirconia (PSZ), the controlled variables included sintering temperature, duration time, heating rate, cooling rate, quenching temperature, and isothermal treatment time, etc. Wherein the sintering temperature was 1450 °C with a duration time of 2 h; the heating rate was controlled at the regime of 100 °C/min to 450 °C/min, and the cooling rate ranged from 1 °C/min to 400 °C/min; the quenching temperature ranged from 25 °C to 1450 °C, and the isothermal

treatment time was adjusted at the regime of 0-5 h. After attaining the specific process parameters, the CaO-PSZ ceramics samples were cooled with the microwave furnace and removed out to conduct characterization analysis, further to investigate the influence of microwave sintering on the stability properties and phase structures of CaO-PSZ ceramics.

3 Results and discussion

3.1 Stability properties analysis by XRD characterization

The stability properties of zirconia ceramics materials are usually measured by the stability rate, and the stability rate is defined as Eq. (1) [41, 42]:

$$\text{Stability rate} = \frac{\text{Intensity of } 29.92°}{\text{Intensity of } 28.06° + \text{Intensity of } 31.24° + \text{Intensity of } 29.92°} \times 100\% \quad (1)$$

Where Intensity of 28.06° and Intensity of 31.24° indicate the peak intensities of monoclinic phase zirconia (m-ZrO_2); Intensity of 29.92° denotes the peak intensity of cubic phase zirconia (c-ZrO_2).

Based on the XRD patterns, the stability rate can be calculated by Eq. (1). Consequently, effects of experimental variable factors on the phase structures and stability properties of the CaO-PSZ ceramics were systematically investigated, including heating rate, cooling rate, quenching temperature, and isothermal treatment time, further to determine the optimum preparation process parameters for CaO-PSZ ceramics by microwave sintering.

3.1.1 Effect of heating rate on stability rate

The effects of heating rate on the phase structures of the CaO-PSZ ceramics samples were shown in Fig. 3, obtained at controlling the maximum temperature at 1450 °C with the heating rate regime of 100 °C/min to 450 °C/min, the holding time of 2 h, the cooling rate of

4 °C/min and quenching treatment at 950 °C. As observed from Fig. 3, as the heating rate increased from 100 °C/min to 450 °C/min, the heating rate showed little effect on the phase structure of CaO-PSZ ceramics, similarly with the same mixed phase structure composed by cubic phase zirconia (c-ZrO_2) and monoclinic phase zirconia (m-ZrO_2), indicating the formation of CaO-PSZ ceramics; and the intensity of each diffraction peak was relatively unchanged, including the diffraction peak of cubic phase zirconia (c-ZrO_2) at 29.92° and the diffraction peaks of monoclinic phase zirconia (m-ZrO_2) at 28.06° and 31.24°. Moreover, compared with the XRD pattern of fused zirconia (Fig. 1), the new phase, monoclinic phase zirconia (m-ZrO_2) appeared in the CaO-PSZ ceramics samples, which was attributed to the reversible martensitic transformation of zirconia [11,12]. Wherein pure zirconia maintains the monoclinic phase (m-ZrO_2) at room temperature, while it will be transformed into tetragonal phase zirconia (t-ZrO_2) at temperatures higher than 1173 °C, and transformed into cubic phase zirconia (c-ZrO_2) at 2370 °C and becomes a liquid phase at 2690 °C [13]. The reversible martensitic transformation of zirconia material is mainly related to the phase conversion temperature, hence showing the little relationship with the heating rate. Therefore, at the temperature regime of 1450 °C to 950 °C, the conversion of cubic phase zirconia (c-ZrO_2) to tetragonal phase zirconia (t-ZrO_2) and the conversion of tetragonal phase zirconia (t-ZrO_2) to monoclinic phase zirconia (m-ZrO_2) occurred, rendering that the cubic phase zirconia (c-ZrO_2) was partially converted into monoclinic phase zirconia (m-ZrO_2).

Based on the XRD pattern plotted in Fig. 3, the effects of heating rate on the stability rate were determined in Fig. 4. As seen from Fig. 4, the high heating rates rendered the small influence on the fluctuation of the stability rate, with 70.7% at 100 °C/min slowly improved

to 71.2% at 250 °C/min and 71.3% at 450 °C/min, which the results were consistent with findings obtained from the XRD pattern (Fig. 3). Therefore, it can be considered that the heating rate had little influence on the stability properties of the CaO-PSZ ceramics, and a higher heating rate can be selected to reduce the preparation time by microwave sintering.

3.1.2 Effect of cooling rate on stability rate

The effects of cooling rate on the phase structures of the CaO-PSZ ceramics samples were presented in Fig. 5, obtained at controlling the maximum temperature at 1450 °C with the heating rate of 4 °C/min, the holding time of 2 h, and quenching treatment at 950 °C with the cooling rate regime of 1 °C/min to 400 °C/min. As observed from Fig. 5, as the cooling rate increased from 2 °C/min to 8 °C/min, the intensity of the diffraction peak of cubic phase zirconia (c-ZrO_2) at 29.92° increased sharply, and the intensities of the diffraction peaks of monoclinic phase zirconia (m-ZrO_2) at 28.06° and 31.24° also increased; while increased from 8 °C/min to 20 °C/min even increased to 400 °C/min, the intensity of the diffraction peak of cubic phase zirconia (c-ZrO_2) at 29.92° still maintained a substantial increase, but the intensities of the diffraction peaks of monoclinic phase zirconia (m-ZrO_2) at 28.06° and 31.24° decreased. The change of the phase structure of the CaO-PSZ ceramics samples indicated the cooling rate rendered the significant influence on the phase structure of the CaO-PSZ ceramics samples, and increasing cooling rate improved the transformation rate of the conversion of tetragonal phase zirconia (t-ZrO_2) to monoclinic phase zirconia (m-ZrO_2), which was ascribed to that during the cooling process, with temperature decreased from 1450 °C to 1173 °C, a faster cooling rate naturally implicated a greater internal motivation to the phase conversion of tetragonal phase zirconia (t-ZrO_2) to monoclinic phase zirconia

(m-ZrO_2) [13]; meanwhile, the optimal cooling rate would be between 8 °C/min and 20 °C/min.

Based on the XRD pattern plotted in Fig. 5, the effects of cooling rate on the stability rate were determined in Fig. 6. As observed from Fig. 6, the stability rate improved with the cooling rate increasing, with 41.7% with a cooling rate of 1 °C/min improved to 90.8% with a cooling rate of 20 °C/min; exceeding 20 °C/min, the change trend of the stability rate with cooling rate gradually became slower and tended to be balanced, with 92.9% at a cooling rate of 40 °C/min slowly increased to 96.5% at a cooling rate of 400 °C/min, indicating decreasing the cooling rate was beneficial for the crystal conversion of cubic phase zirconia (c-ZrO_2) to monoclinic phase zirconia (m-ZrO_2). Therefore, it is necessary to cool with a slow cooling rate in order to obtain a lower stability rate, referring to the more formation of partially stabilized zirconia (PSZ). The slower cooling rate caused the lower stability properties, rendering the more the monoclinic phase zirconia (m-ZrO_2) be formed.

3.1.3 Effect of quenching temperature on stability rate

The effects of quenching temperature on the phase structures of the CaO-PSZ ceramics samples were illustrated in Fig. 7, obtained at controlling the maximum temperature at 1450 °C with the heating rate of 400 °C/min, the holding time of 2 h, and cooled with the cooling rate of 4 °C/min to different quenching temperature treatment, ranging from 1400 °C to 25 °C. As observed from Fig. 7, with the quenching temperature decreased from 1450 °C to 950 °C, the intensity of the diffraction peak of cubic phase zirconia (c-ZrO_2) at 29.92° presented a decreasing trend, and the intensity of the diffraction peaks of monoclinic phase zirconia (m-ZrO_2) at 28.06° and 31.24° increased continuously, indicating the continuous

completion of the phase conversion, including the cubic phase zirconia (c-ZrO_2) to tetragonal phase zirconia (t-ZrO_2) and the tetragonal phase zirconia (t-ZrO_2) to monoclinic phase zirconia (m-ZrO_2); while temperatures lower than 950 °C, the intensities of the diffraction peaks of zirconia phases were unchanged, presenting little effect on the phase structures of CaO-PSZ samples. Therefore, it can be concluded that the optimal quenching temperature can be chosen at 950 °C. The conversion temperature of tetragonal phase zirconia (t-ZrO_2) to monoclinic phase zirconia (m-ZrO_2) occurs at 1173 °C [13]; and with temperature decreasing, the phase conversions continuously completed, including the cubic phase zirconia (c-ZrO_2) to tetragonal phase zirconia (t-ZrO_2) and the tetragonal phase zirconia (t-ZrO_2) to monoclinic phase zirconia (m-ZrO_2), rendering the continue conversion of cubic phase zirconia (c-ZrO_2) and the formation of monoclinic phase zirconia (m-ZrO_2), further representing by the increase of the intensity of monoclinic phase zirconia (m-ZrO_2) diffraction peaks and the decrease of the intensity of cubic phase zirconia (c-ZrO_2) diffraction peak.

Based on the XRD pattern plotted in Fig. 7, the effects of quenching temperature on the stability rate were plotted in Fig. 8. As observed from Fig. 8, at the early stage of the decrease process of quenching temperature, the stability rate of the CaO-PSZ samples presented a decreasing trend, and this trend was more obvious in the high-temperature zone, with 97.4% at 1450 °C reduced to 71.2% at 950 °C; as the temperature continuously decreased to lower than 950 °C, the change of the stability of zirconia tended to be gentle, and the stability rate of zirconia samples did not change substantially and tended to balance with the temperature further decreased, with 71.2% at 950 °C changed to 70.2% at 25 °C. The phenomenon indicated that during the cooling process, the lower the quenching temperature, the more

difficult the phase transition occurred; meanwhile, it can be speculated that the sufficient low temperature will inhibit the phase transition in zirconia samples. Moreover, the optimal quenching temperature can be chosen at 950 °C, which was consistent with the finding obtained from Fig. 7.

3.1.4 Effect of isothermal treatment time on stability rate

The effects of isothermal treatment time on the phase structures of the CaO-PSZ ceramics samples were displayed in Fig. 9, obtained at controlling the maximum temperature at 1450 °C with the heating rate of 400 °C/min, the holding time of 2 h, followed by cooled to a specific temperature and kept warm with holding time ranging from 0 h to 5 h, finally with quenching treatment. As observed from Fig. 9(a), during the cooling process, the isothermal treatment time at 1300 °C had little influence on the phase structures, representing by the intensity of diffraction peak of cubic phase zirconia at 29.92° and monoclinic zirconia phase at 28.06° and 31.24° unchanged. Moreover, the same findings were obtained from Fig. 9(b) and Fig. 9(c), the isothermal treatment time at 1100 °C and 900 °C also presented little influence on the phase structures. Therefore, it can be concluded that during the cooling process, the isothermal treatment time at a certain temperature rendered little influence on the phase structures of the CaO-PSZ ceramics. The reversible martensitic transformation of zirconia material is mainly influenced by the phase conversion temperatures, without connection with the isothermal treatment time.

Based on the XRD pattern shown in Fig. 9, the effects of isothermal treatment time on the stability rate were presented in Fig. 10. As observed from Fig. 10, at a quenching temperature of 1300 °C, the stability rate decreased from 90.6% without isothermal treatment

to 88.4% with 5 h; at 1100 °C, the stability rate decreased from 79.1% without isothermal treatment to 78.3% with 5 h; at 900 °C, the stability rate decreased from70.7% without isothermal treatment to 69.8% with 5 h. During the cooling process, after temperature decreased to a certain point, conducting the isothermal ageing treatment cannot render the significant contribution to the increase of the monoclinic phase zirconia (m-ZrO_2); conversely, the changing trend of the stability rate reached balanced. Therefore, the isothermal ageing treatment conducted in the cooling process cannot promote the phase transformation of zirconia samples, further to reduce the stability properties of the CaO-PSZ ceramics.

3.2 Characterization by SEM

SEM patterns of zirconia material before and after microwave sintering were illustrated in Fig. 11, wherein the SEM patterns of the zirconia sample before sintering were presented in Fig. 11(a)-(c), the SEM patterns of the prepared CaO-PSZ ceramics sintered at 1450 °C for 2.0 h were displayed in Fig. 11(d)-(f).

For the fused zirconia raw material, as observed from Fig. 11(a)-(b), the grain boundaries were regular and distinct, and the angles for the boundary intersection points were almost balanced at 120°, indicating that the raw material was mainly composed by cubic phase zirconia (c-ZrO_2) with fluorite structure, which the result was consistent with finding obtained from Fig. 1. Meanwhile, as seen from Fig. 11(c), the surface of fused zirconia raw material was filled with scaly, which were overlapped together, without fatal crystal structure defects observed, such as cracks, holes and pits.

In addition, for the prepared CaO-PSZ ceramic samples, as displayed in Fig. 11(d)-(f), the more dense structure with no cracks appeared on the whole surface, and the acicular

patterns of grains and fine round particles gathered at the crystal boundary (Fig. 11(d)-(e)). Wherein the aggregation phenomenon of acicular grains and fine particles at the grain boundary was attributed to that the precipitation behavior of the CaO stabilizer. Moreover, compared with Fig. 11(b) and Fig. 11(e), the complete cubic-phase zirconia was observed to disappear and changed to a mixed-phase structure, indicating the formation of the CaO-PSZ ceramics.

3.3 Characterization by EDAX

The SEM pattern and EDAX spectra of the CaO-PSZ ceramics sample prepared at 1450 °C for 2 h by microwave sintering were displayed in Fig. 12, wherein Fig. 12(a) illustrated the microscopic appearance, Fig. 12(b)-(d) displayed the elemental semi-quantitative analysis of spot 2, spot 4, and spot 5, respectively. As observed from Fig. 12(a), spot 2 was located at the grain boundary, and the locations of spot 4 and spot 5 were different with spot 2; hence, there existed obvious difference for the elemental compositions with spot 2 compared to spot 4 and spot 5. Wherein spot 2 was determined with the 12.81% of CaO content and 18.67% of ZrO_2 content, while spot 4 was characterized by the 3.06% of CaO content and 68.45% of ZrO_2 content, and spot 5 was characterized by the 3.10% of CaO content and 71.50% of ZrO_2 content. Obviously, the CaO content at spot 2 with 12.81% was much higher than that at spot 4 and spot 5, with 3.06% at spot 4 and 3.10% at spot 5, respectively; meanwhile, the ZrO_2 content at spot 2 with 18.67% was much lower than that at spot 4 and spot 5, with 68.45% at spot 4 and 71.50% at spot 5, respectively, which the great difference for elemental composition distribution clearly verified the precipitation behavior of the CaO stabilizer at the grain boundary, further signifying the formation of the CaO-PSZ

ceramics. Moreover, the findings obtained from the EDAX analysis were consistent with the SEM analysis.

4 Conclusions

In this work, the microstructure and stability properties of calcium oxide-partially stabilized zirconia (CaO-PSZ) ceramics were systematically studied, with fused zirconia as raw material prepared by microwave sintering. Results indicated that during the sintering preparation process, the intensity of the diffraction peak of cubic phase zirconia (c-ZrO_2) at 29.92° decreased, and the intensity of the diffraction peaks of monoclinic phase zirconia (m-ZrO_2) at 28.06° and 31.24° increased, which was ascribed to the reversible martensitic transformation of zirconia. Meanwhile, the influence of various factors on zirconia stability properties presented great difference, representing by the stability rate synchronously improved with the increase of heating rate, cooling rate and quenching temperature, while without significant connection with isothermal treatment time. Moreover, SEM and EDAX characterization signified the precipitation behavior of CaO stabilizer at the crystal boundary, with the acicular grains and fine particles formed, indicating the formation of CaO-PSZ ceramics. The work highlights the effective synthesis of CaO-PSZ ceramics from fused zirconia by microwave sintering, even extending to other advanced ceramics materials and refractory materials.

Acknowledgments

Financial support from the National Natural Science Foundation of China (Grant No. 51764052) and Innovative Research Team (in Science and Technology) in University of Yunnan Province.

References

1. L.A. Bicalho, C.A.R.P. Baptista, R.C. Souza, C. Santos, K. Strecker, M.J.R. Barboza, Fatigue and subcritical crack growth in ZrO_2-bioglass ceramics, Ceram. Int. 39(3) (2013) 2405-2414. https://doi.org/10.1016/j.ceramint.2012.08.093.
2. F. A. Kroger, Electronic conductivity of calcia-stabilized zirconia, J. Am. Ceram. Soc. 49(4) (2010) 215-218. https://doi.org/10.1111/j.1151-2916.1966.tb13237.x.
3. A.K. Pandey, K. Biswas, Influence of sintering parameters on tribological properties of ceria stabilized zirconia bio-ceramics, Ceram. Int. 2011, 37(1) (2011) 257-264. https://doi.org/10.1016/j.ceramint.2010.08.041.
4. D.K. Leung, C.J. Chan, M. Rühle, F.F. Lange, Metastable crystallization, phase partitioning, and grain growth of ZrO_2-Gd_2O_3 materials processed from liquid precursors, J. Am. Ceram. Soc. 74(11) (2005) 2786-2792. https://doi.org/10.1111/j.1151-2916.1991.tb06844.x.
5. W.P. Halperin, Quantum size effects in metal particles, Rev. Mod. Phys. 58(3) (1986) 533-606. https://doi.org/10.1103/RevModPhys.58.533.
6. Z.Q. Guo, B.Q. Han, H. Dong, Effect of coal slag on the wear rate and microstructure of the ZrO_2-bearing chromia refractories, Ceram. Int. 23(6) (1997) 489-496. https://doi.org/10.1016/S0272-8842(96)00059-4.

7. S. Bhargava, H. Doi, R. Kondo, H. Aoki, H. Takao, K. Shohei, Effect of sandblasting on the mechanical properties of Y-TZP zirconia, Bio-med. Mater. Eng. 22(6) (2012) 383-398. https://doi.org/10.3233/BME-2012-0727.

8. C. Patapy, F. Gouraud, M. Huger, R. Guinebretière, B. Ouladiaff, D. Chateigner, T. Chotard, Investigation by neutron diffraction of texture induced by the cooling process of zirconia refractories, J. Eur. Ceram. Soc. 34(15) (2014) 4043-4052. https://doi.org/10.1016/j.jeurceramsoc.2014.05.027.

9. P.E. Reyes-Morel, I.W. Chen, Transformation plasticity of CeO_2-stabilized tetragonal zirconia polycrystals: I, stress assistance and autocatalysis, J. Am. Ceram. Soc. 71(5) (2010) 343-353. https://doi.org/10.1111/j.1151-2916.1988.tb05052.x.

10. L.L. Fehrenbacher, L.A. Jacobson, Metallographic observation of the monoclinic-tetragonal phase transformation in ZrO_2, J. Am. Ceram. Soc. 2010, 48(3) (2010) 157-161. https://doi.org/10.1111/j.1151-2916.1965.tb16054.x.

11. M.J. Readey, A.H. Heuer, R.W. Steinbrech, Annealing of test specimens of high-toughness magnesia-partially-stabilized zirconia, J. Am. Ceram. Soc. 71(1) (2010) 2-6. https://doi.org/10.1111/j.1151-2916.1988.tb05766.x.

12. S. Guo, Y. Kagawa, Isothermal and cycle properties of EB-PVD yttria-partially-stabilized zirconia thermal barrier coatings at 1150 and 1300 °C, Ceram. Int. 33(3) (2007) 373-378. https://doi.org/10.1016/j.ceramint.2005.10.005.

13. R.H.J. Hannink, P.M. Kelly, B.C. Muddle, Transformati on toughening in zirconia-containing ceramics, J. Am. Ceram. Soc. 83(3) (2002) 461-487. https://doi.org/10.1111/j.1151-2916.2000.tb01221.x.

14. R.G. Garvie, R.H. Hannink, R.T. Pascoe, Ceramic steel, Nature. 258 (1975) 703-704. https://doi.org/10.1038/258703a0.

15. K.Q. Li, J. Chen, J.H. Peng, S. Koppala, M. Omran, G. Chen, One-step preparation of CaO-doped partially stabilized zirconia from fused Zirconia, Ceram. Int. https://doi.org/10.1016/j.ceramint.2019.11.129.

16. M.W. Yan, Y. Li, G.X. Yin, S.H. Tong, J.H. Chen, Synthesis and characterization of a MgO-$MgAl_2O_4$-ZrO_2, composite with a continuous network microstructure, Ceram. Int. 43(8) (2017) 5914-5919. https://doi.org/10.1016/j.ceramint.2017.01.082.

17. X.L. Han, Z.Z. Liang, L. Feng, W. Wang, J.F. Chen, C.Y. Xu, H. Zhao, Co-precipitated synthesis of Al_2O_3-ZrO_2 composite ceramic nanopowders by precipitant and drying method regulation: A systematic study, Ceram. Int. 41(1) (2015) 505-513. https://doi.org/10.1016/j.ceramint.2014.08.098.

18. J.P. Luan, J.D. Zhang, X.M. Yao, F. Li, B.X. Jia, Controlled synthesis and growth mechanism of Bi_2O_3/YSZ solid electrolyte materials, Ceram. Int. 42(14) (2016) 16262-16265. https://doi.org/10.1016/j.ceramint.2016.07.160.

19. Y.J. Xia, J.L. Song, D.N. Yuan, X.N. Guo, X. Guo, Synthesis and characterization of one-dimensional metal oxides: TiO_2, CeO_2, Y_2O_3-stabilized ZrO_2 and $SrTiO_3$, Ceram. Int. 41(1) (2015) 533-545. https://doi.org/10.1016/j.ceramint.2014.08.102.

20. L.Q. Kong, S.Y. Zhu, Q.L. Bi, Z.H. Qiao, J. Yang, W.M. Liu, Friction and wear behavior of self-lubricating $ZrO_2(Y_2O_3)$-CaF_2-Mo-graphite composite from 20°C to 1000°C, Ceram. Int. 40(7) (2014) 10787-10792. https://doi.org/10.1016/j.ceramint.2014.03.068.

21. A. Bogicevic, C. Wolverton, G.M. Crosbie, E.B. Stechel, Defect ordering in aliovalently doped cubic zirconia from first principles. Phys. Rev. B. 64(1) (2001) 014106. https://doi.org/10.1103/PhysRevB.64.014106.

22. R.C. Garvie, Structure and thermomechanical properties of partially stabilized zirconia in the CaO-ZrO_2 system, J. Am. Ceram. Soc. 55 (2010) 152-157. https://doi.org/10.1007/978-94-009-0741-6_15.

23. H. Wang, M.H. Wang, W.Y. Zhang, N. Zhao, W. Wei, Y.H. Sun, Synthesis of dimethyl carbonate from propylene carbonate and methanol using CaO-ZrO_2 solid solutions as highly stable catalysts, Catal. Today. 115(1) (2006) 107-110. https://doi.org/10.1016/j.cattod.2006.02.031.

24. H. Wang. M.H Wang, N. Zhao, W. Wei, Y. Sun, CaO-ZrO_2 solid solution: a highly stable catalyst for the synthesis of dimethyl carbonate from propylene carbonate and methanol, Catal. Lett. 105(3-4) (2005) 253-257. https://doi.org/10.1007/s10562-005-8699-0.

25. K.Q. Li, J. Chen, J.H. Peng, R. Ruan, C. Srinivasakannan, G. Chen, Pilot-scale study on enhanced carbothermal reduction of low-grade pyrolusite using microwave heating, Powder. Technol. https://doi.org/10.1016/j.powtec.2019.11.015.

26. K.Q. Li, G. Chen, J. Chen, J.H. Peng, R. Ruan, C. Srinivasakannan, Microwave pyrolysis of walnut shell for reduction process of low-grade pyrolusite, Bioresource. Technol. 291 (2019) 121838. https://doi.org/10.1016/j.biortech.2019.121838.

27. K.H. Chen, J.H. Peng, C. Srinivasakannan, S.H. Yin, S.H. Guo, L.B. Zhang, Effect of temperature on the preparation of yttrium oxide in microwave field, J. Alloy. Compd. 742 (2018) 13-19. https://doi.org/10.1016/j.jallcom.2018.01.258.

28. K.Q. Li, J. Chen, J.H. Peng, R. Ruan, M. Orman, G. Chen, Dielectric properties and thermal behavior of electrolytic manganese anode mud in microwave field, J. Hazard. Mater. 381 (2020) 121227. https://doi.org/10.1016/j.jhazmat.2019.121227.

29. S. Cheng, Q. Chen, H.Y. Xia, L.B. Zhang, J.H. Peng, X. Jiang, Q. Zhang, Microwave one-pot production of ZnO/Fe_3O_4/activated carbon composite for organic dy

e removal and the pyrolysis exhaust recycle, J. Clean. Prod. 188 (2018) 900-910. https://doi.org/10.1016/j.jclepro.2018.03.308.

30. H.Y. Li, S.W. Li, C. Srinivasakannan, S.H., Yin, J.H., Peng, L.B. Zhang, K. Yang, Microwave regeneration of spent catalyst coupled with ultrasound augmented copper impregnation as a potential adsorbent photocatalyst, Mater. Res. Express. 6 (2018) 045608-045618. https://doi.org/10.1088/2053-1591/aafa09.
31. S.H. Guo, J.H. Peng, G. Chen, L.B. Zhang, S.M. Zhang, Microwave-absorbing characteristics and temperature rising behavior of fused zirconia in microwave field, J. Cent. South. U. Sci. T. (4) (2009) 915-920. https://doi.org/CNKI:SUN:ZNGD.0.2009-04-015.
32. S.H. Guo, G. Chen, J.H. Peng, J. Chen, J.L. Mao, D.B. Li, L.J. Liu, Preparation of partially stabilized zirconia from fused zirconia using roasting, J. Alloy. Compd. 506(1) (2010) L5-L7. https://doi.org/10.1016/j.jallcom.2010.06.156.
33. M.Y. Zhang, L. Gao, J.X. Kang, J. Pu, J.H. Peng, M. Omran, G. Chen, Stability optimisation of CaO-doped partially stabilised zirconia by microwave sintering, Ceram. Int. 45(17) (2019) 23278-23282. https://doi.org/10.1016/j.ceramint.2019.08.024.
34. M. Mazaheri, A.M. Zahedi, M.M. Hejazi. Processing of nanocrystalline 8 mol% yttria-stabilized zirconia by conventional, microwave-assisted and two-step sintering, Mat. Sci. Eng. A-struct. 492(1) (2008) 261-267. https://doi.org/10.1016/j.msea.2008.03.023.
35. R.R. Thridandapani, C.E. Folgar, A. Kulp, D.C. Folz, D.E. Clark, Effect of direct microwave sintering on structure and properties of 8 Mol% Y_2O_3-ZrO_2, Int. J. Appl. Ceram. Tec. 8(5) (2011) 1229-1236. https://doi.org/10.1111/j.1744-7402.2010.02570.x.
36. K.H. Chen, Y. He, C. Srinivasakannan, S.W. Li, S.H. Yin, J.H. Peng, S.H. Guo, L.B. Zhang,

Characterization of the interaction of rare earth elements with P507 in a microfluidic extr action system using spectroscopic analysis, Chem. Eng. J. 356 (2018) 453-460. https://doi.org/10.1016/j.cej.2018.09.039.

37. K.Q. Li, G. Chen, X.T. Li, J.H. Peng, R. Ruan, M. Omran, J. Chen, High-temperature dielectric properties and pyrolysis reduction characteristics of different biomass-pyrolusite mixtures in microwave field, Bioresource. Technol. 294 (2019) 122217. https://doi.org/10.1016/j.biortech.2019.122217.
38. H.Y. Li, H.L. Long, L.B. Zhang, S.H. Yin, S.W. Li, F. Zhu, H.M. Xie, Effectiveness of microwave-assisted thermal treatment in the extraction of gold in cyanide tailings, J. Hazard. Mater. (2019) 121456. https://doi.org/10.1016/j.jhazmat.2019.121456.
39. K.Q. Li, J. Chen, G. Chen, J.H. Peng, R. Ruan, C. Srinivasakannan, Microwave dielectric properties and thermochemical characteristics of the mixtures of walnut shell and manganese ore, Bioresource. Technol. 286 (2019) 121381. https://doi.org/10.1016/j.biortech.2019.121381.
40. Q.X. Ye, J.J. Ru, J.H. Peng, G. Chen, D. Wang, Formation of multiporous MnO/N-doped carbon configuration via carbonthermal reduction for superior electrochemical properties, Chem. Eng. J. 331 (2018) 570-577. https://doi.org/10.1016/j.cej.2017.09.031.
41. L.L. Sun, H.B. Guo, H. Peng, S.K. Gong, H.B. Xu, Influence of partial substitution of Sc_2O_3 with Gd_2O_3 on the phase stability and thermal conductivity of Sc_2O_3-doped ZrO_2, Ceram. Int. 39(3) (2013) 3447-3451. https://doi.org/10.1016/j.ceramint.2012.09.100.
42. Y. Murase, E. Kato, K. Daimon, Stability of ZrO_2 phases in ultrafine ZrO_2-Al_2O_3 mixtures, J. Am. Ceram. Soc. 69(2) (1986) 83-87. https://doi.org/10.1111/j.1151-2916.1986.tb04706.x.

Figure captions

Fig. 1 XRD pattern of fused zirconia raw material.

Fig. 2 Schematic diagram of microwave high temperature furnace.

Fig. 3 XRD patterns of zirconia material treated with different heating rates.

Fig. 4 Effects of heating rate on stability rate.

Fig. 5 XRD patterns of zirconia material treated with different cooling rates.

Fig. 6 Effects of cooling rate on stability rate.

Fig. 7 XRD patterns of zirconia material treated at different quenching temperatures.

Fig. 8 Effects of quenching temperature on stability rate.

Fig. 9 XRD patterns of zirconia material treated with different isothermal treatment times, (a) 1300 °C; (b) 1100 °C; (c) 900 °C.

Fig. 10 Effects of isothermal treatment time on stability rate, (a) 1300 °C; (b) 1100 °C; (c) 900 °C.

Fig. 11 SEM patterns of zirconia material before and after microwave sintering; (a) raw material, 100×; (b) 200×; (c) 200×; (d) sintered sample, 1000×; (e) 5000×; (f) 5000×.

Fig. 12 SEM pattern and EDAX spectra of zirconia material sintered at 1450 °C for 2 h, (a) SEM pattern; (b) EDAX of spot 2; (c) EDAX of spot 4; (c) EDAX of spot 5.

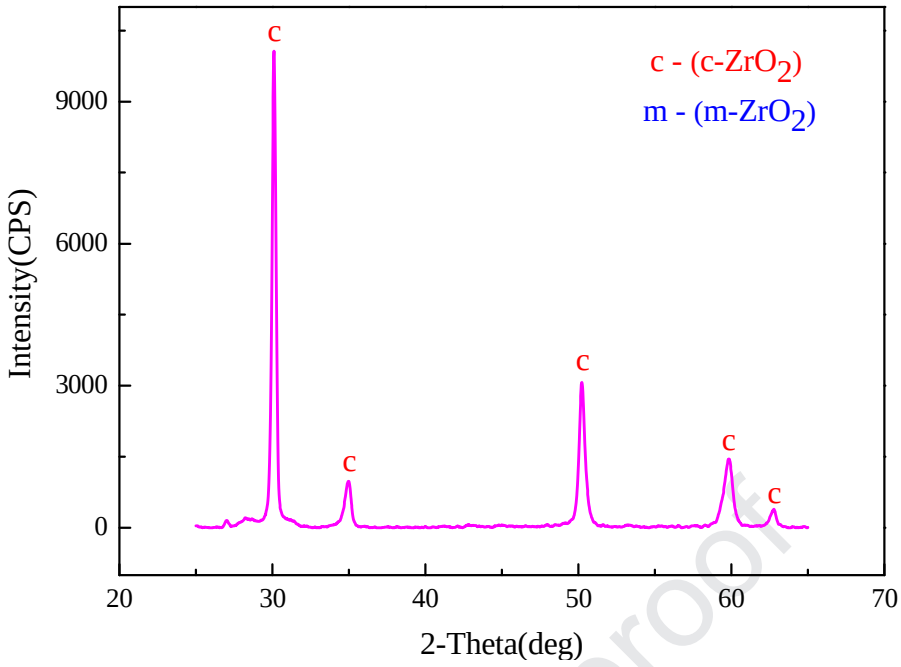

Fig. 1 XRD pattern of fused zirconia raw material.

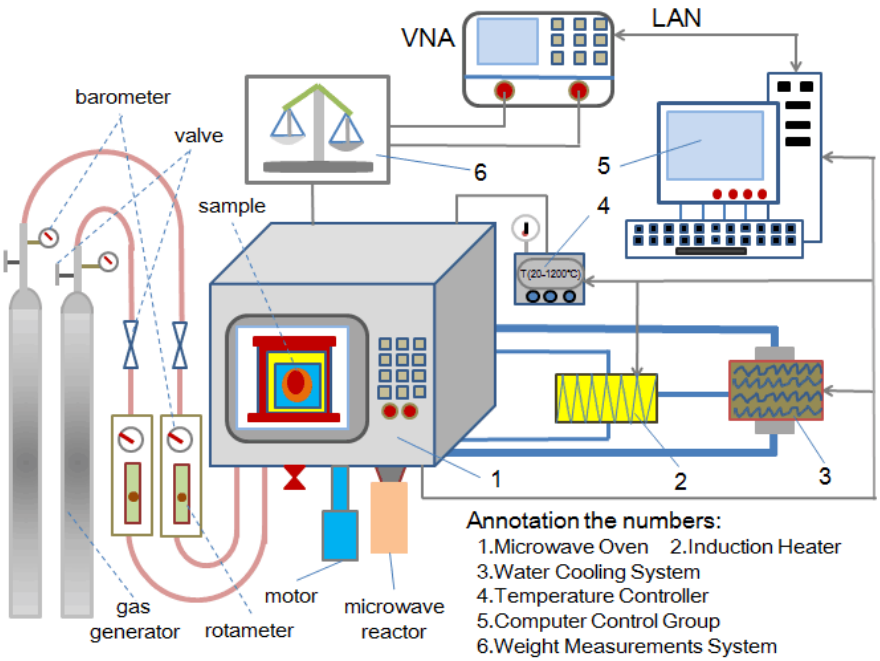

Fig. 2 Schematic diagram of microwave high temperature furnace.

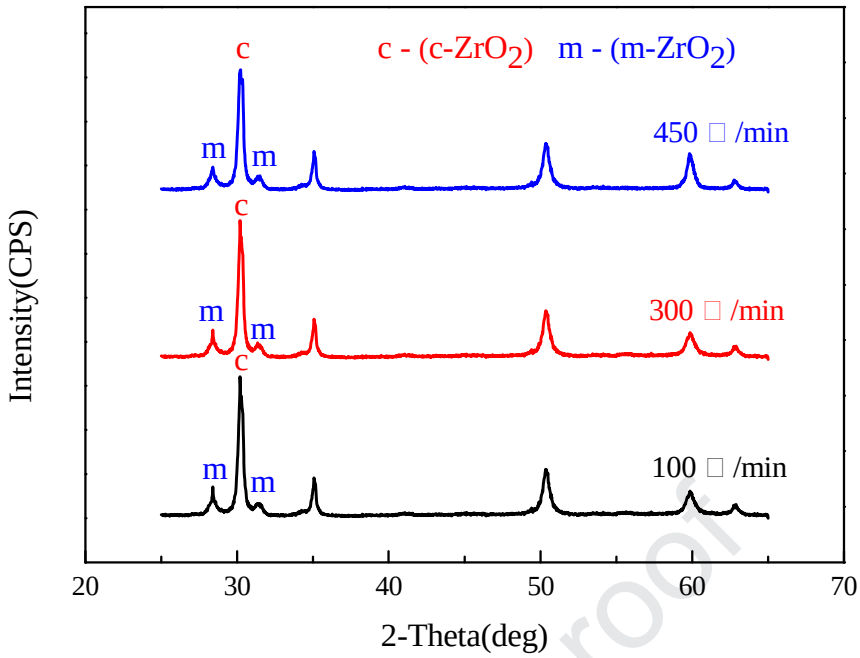

Fig. 3 XRD patterns of zirconia material treated with different heating rates.

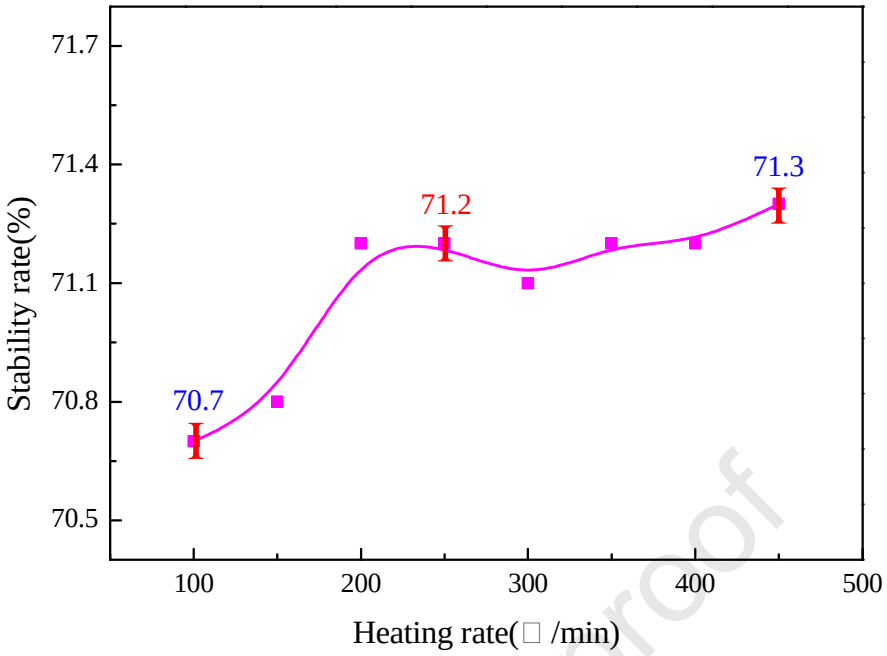

Fig. 4 Effects of heating rate on stability rate.

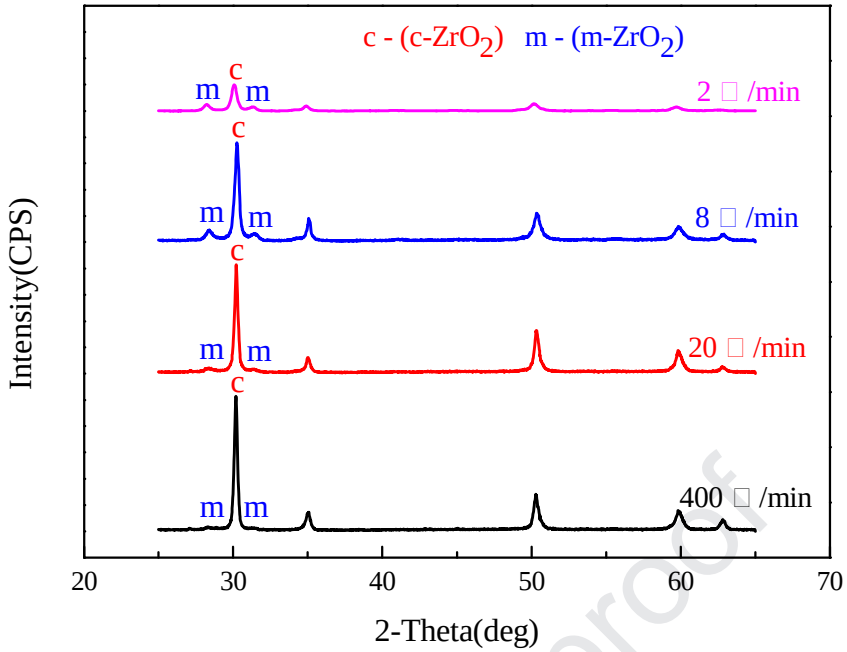

Fig. 5 XRD patterns of zirconia material treated with different cooling rates.

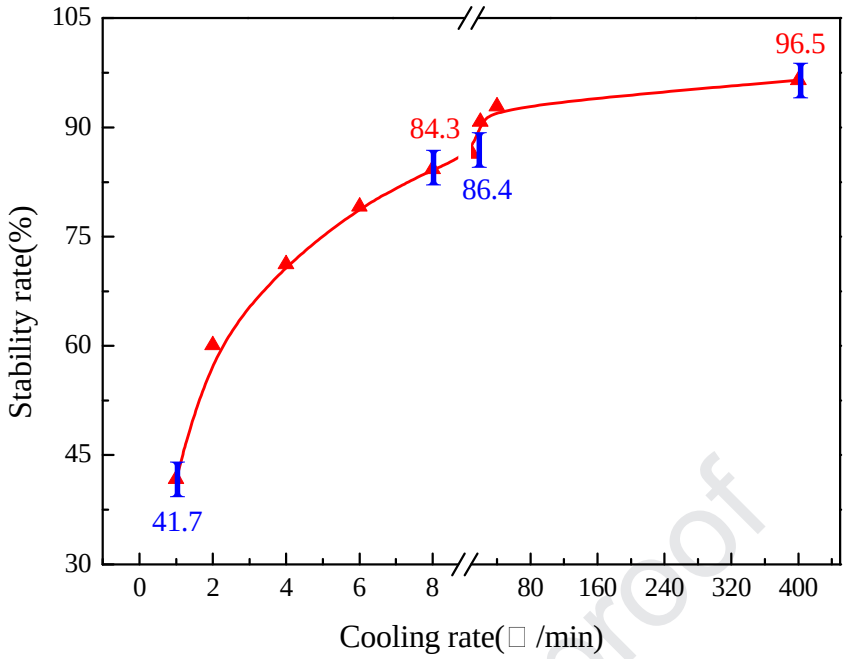

Fig. 6 Effects of cooling rate on stability rate.

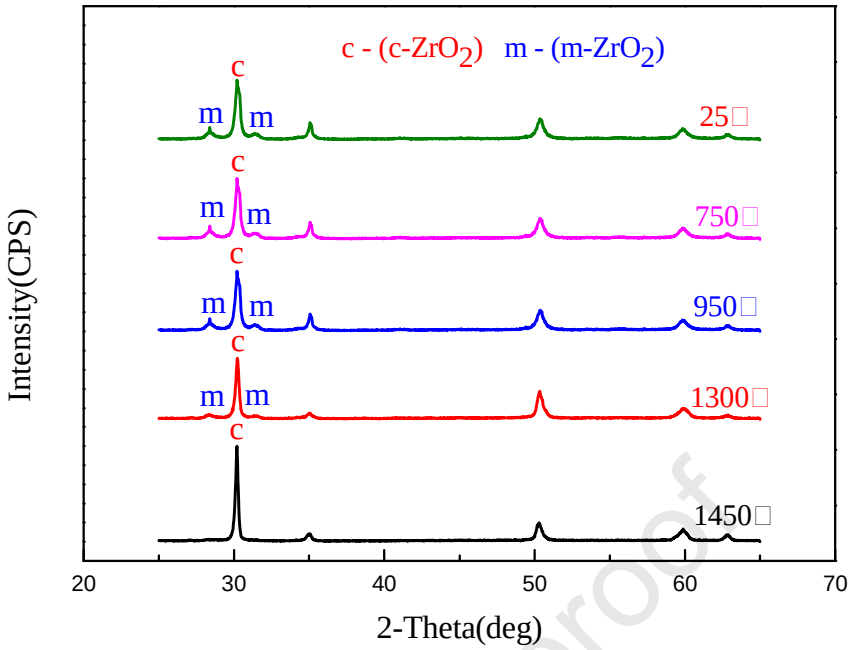

Fig. 7 XRD patterns of zirconia material treated at different quenching temperatures.

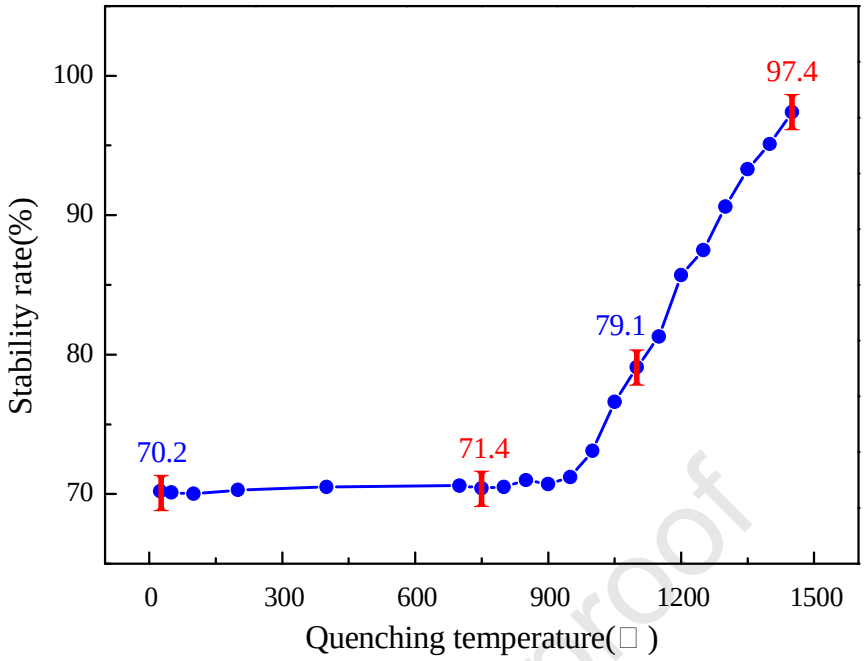

Fig. 8 Effects of quenching temperature on stability rate.

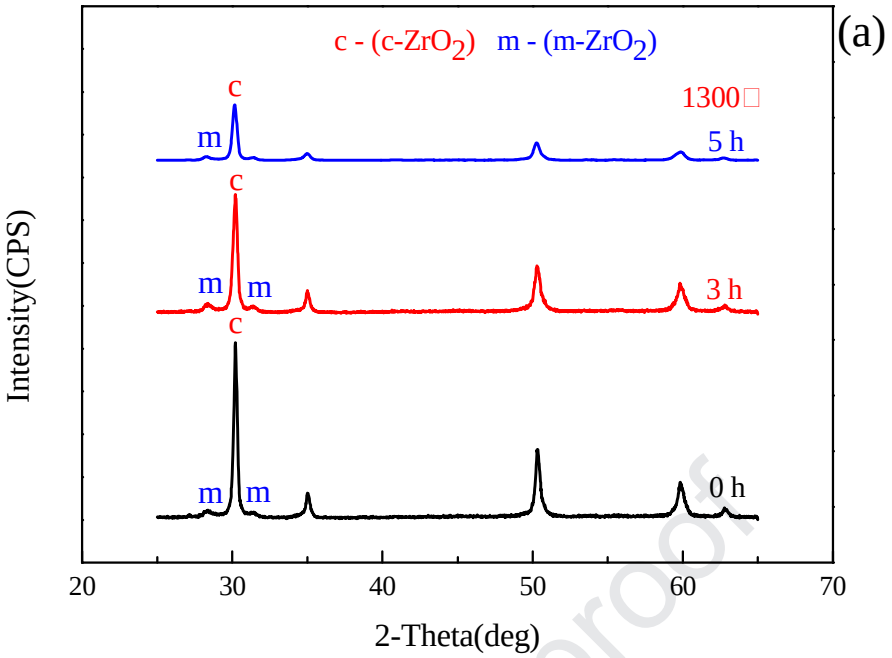

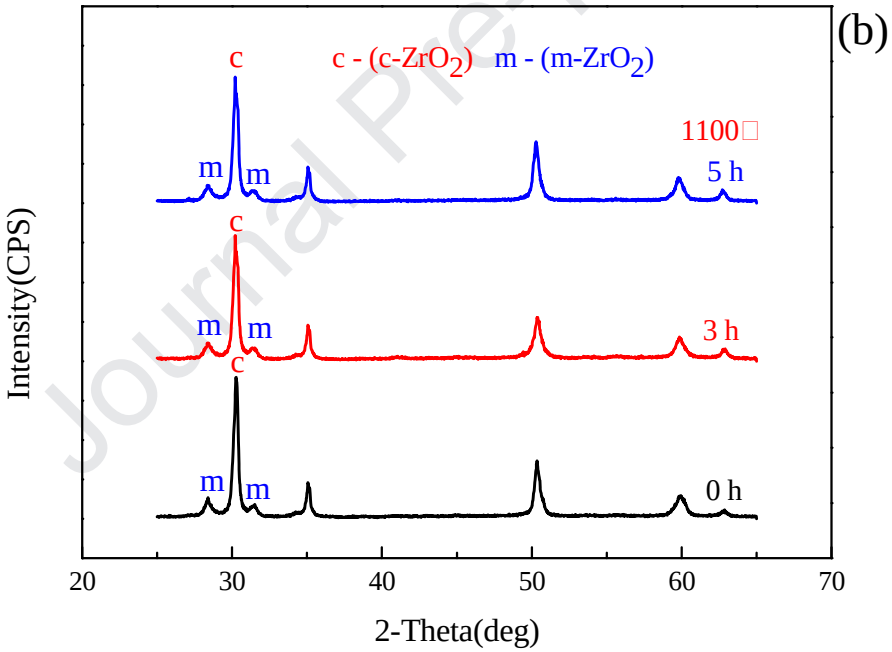

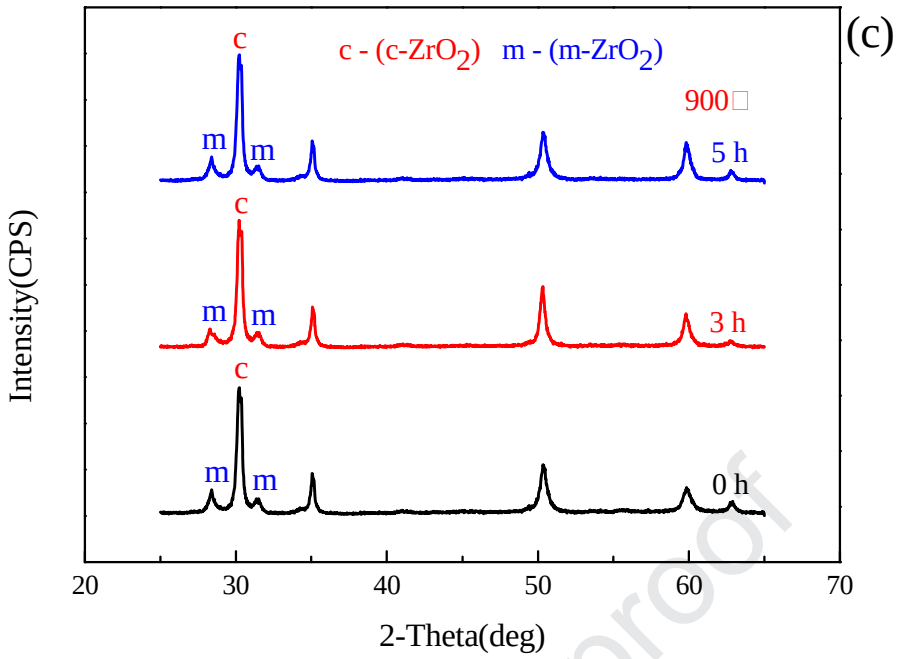

Fig. 9 XRD patterns of zirconia material treated with different isothermal treatment times, (a) 1300 °C; (b) 1100 °C; (c) 900 °C.

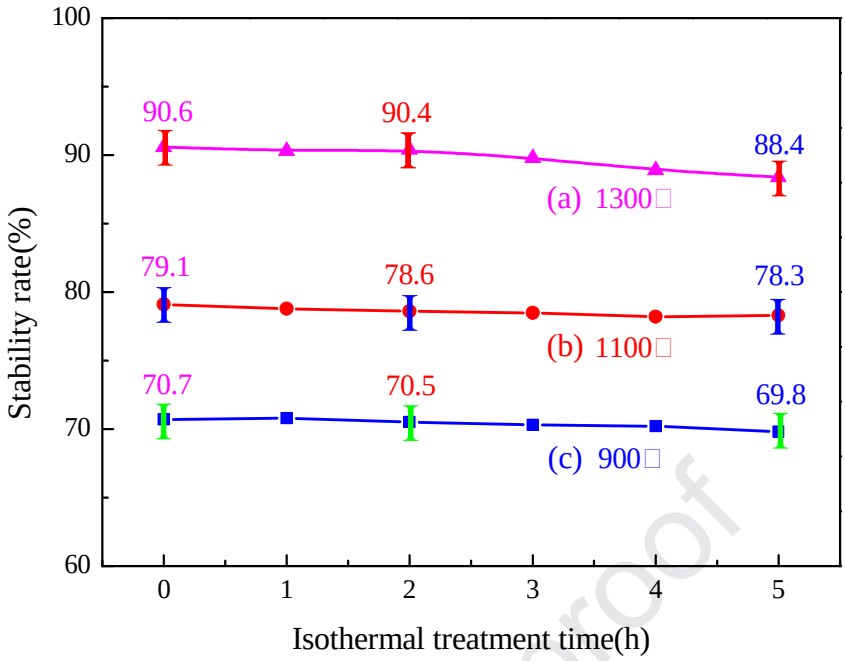

Fig. 10 Effects of isothermal treatment time on stability rate, (a) 1300 °C; (b) 1100 °C; (c) 900 °C.

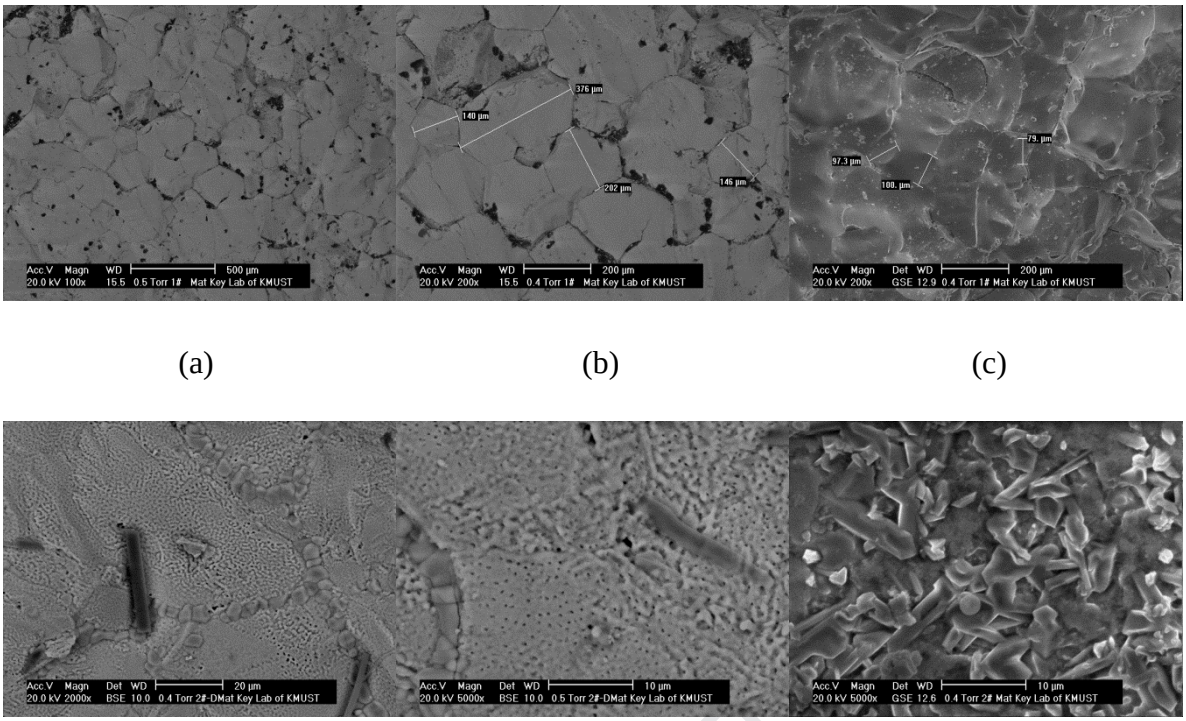

(a) (b) (c)

(d) (e) (f)

Fig. 11 SEM patterns of zirconia material before and after microwave sintering; (a) raw material, 100×; (b) 200×; (c) 200×; (d) sintered sample, 1000×; (e) 5000×; (f) 5000×.

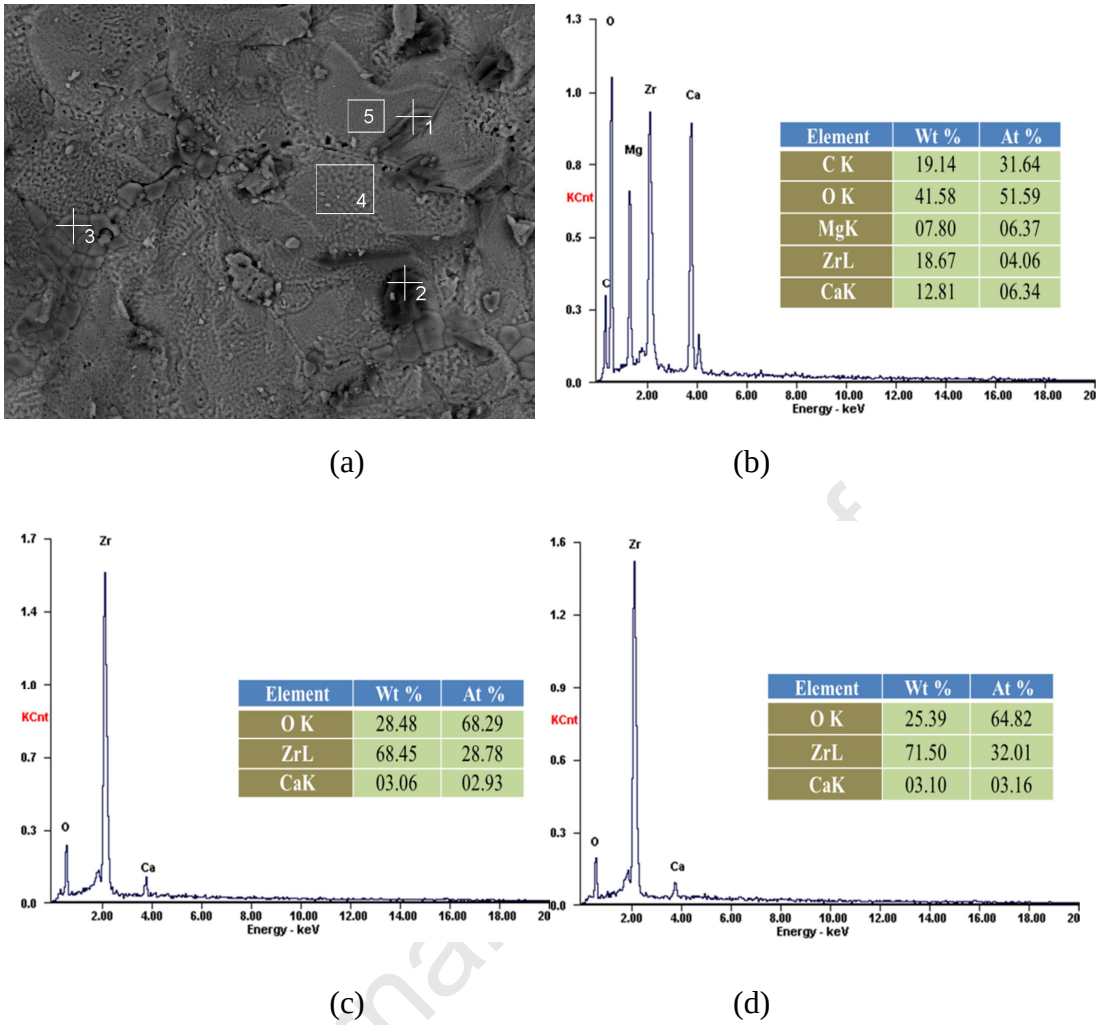

Fig. 12 SEM pattern and EDAX spectra of zirconia material sintered at 1450 °C for 2.0 h, (a) SEM pattern; (b) EDAX of spot 2; (c) EDAX of spot 4; (c) EDAX of spot 5.

Declaration of interests

☒ The authors declare that they have no known competing financial interests or personal relationships that could have appeared to influence the work reported in this paper.

☐The authors declare the following financial interests/personal relationships which may be considered as potential competing interests: